Hindawi
Journal of Chemistry
Volume 2021, Article ID 3475036, 10 pages
https://doi.org/10.1155/2021/3475036

Research Article

Phytogenic Synthesis and Characterization of NiO-ZnO Nanocomposite for the Photodegradation of Brilliant Green and 4-Nitrophenol

Sirajul Haq,[1] **Aqsa Waheed Raja**,[1] **Sadiq Ur Rehman**,[1] **Amine Mezni**,[2] **Manel Ben Ali**,[3] **Amor Hedfi**,[3] **Muhammad Imran Shahzad**,[4] **Wajid Rehman**,[5] **Nadia Shahzad**,[6] **Muhammad Waseem**,[7] **and Pervaiz Ahmad**[8]

[1]*Department of Chemistry, University of Azad Jammu and Kashmir, Muzaffarabad 13100, Pakistan*
[2]*Department of Chemistry, College of Science, Taif University, P.O. Box 11099, Taif 21944, Saudi Arabia*
[3]*Department of Biology, College of Sciences, Taif University, P.O. Box 11099, Taif 21944, Saudi Arabia*
[4]*Nanosciences and Technology Department (NS & TD), National Center for Physics (NCP), 44000 Islamabad, Pakistan*
[5]*Department of Chemistry, Hazara University Mansehra, Mansehra 21300, Pakistan*
[6]*US-Pakistan Centre for Advanced Studies in Energy, National University of Science and Technology (NUST), 44000 Islamabad, Pakistan*
[7]*Department of Chemistry, COMSATS University Islamabad (CUI), Islamabad, Pakistan*
[8]*Department of Physics, University of Azad Jammu and Kashmir, 13100 Muzaffarabad,, Pakistan*

Correspondence should be addressed to Sirajul Haq; cii_raj@yahoo.com

Received 7 August 2021; Revised 17 September 2021; Accepted 20 September 2021; Published 13 October 2021

Academic Editor: Christos Kordulis

The NiO-ZnO nanocomposite (NiO-ZnO NC) was synthesized by ecofriendly process by using *Diospyros kaki* (*D. kaki*) extract of leaves as reducing and capping agents. X-ray diffraction (XRD) was used for examined crystallinity, cell dimensions, and crystallite size (7.6 nm). To determine the purity of sample and weight percentage, energy dispersive X-ray (EDX) is used. The surface morphology was determined by scanning electron microscopy (SEM) and transmission electron microscopy (TEM). By using Fourier transform infrared spectroscopy (FTIR), functional groups in samples were determined. By using diffuse reflectance data (DRS), band gap energy calculated via Tauc plot was 3.23 eV. The photocatalytic activity was checked against brilliant green (BG) and 4-nitrophenol (4-NP) and 92.5% and 69.7% of brilliant green (BG) and 4-nitrophenol (4-NP) were degraded with rate of degradation which were 0.0281 and 0.011 min^{-1}.

1. Introduction

Due to industrial revolution, environmental pollution exponentially increases with passage of time by releasing carcinogenic and mutagenic hazardous wastes and their side products to aqueous environment [1, 2]. Major contributors of water and air contamination are food, paper, textile, and pharmaceutical industries; among these, textile industries produce many toxic substances, and due to non-biodegradability and stability of organic pollutants, they are considered deadly [3, 4]. Different dyes such as methylene blue, golden yellow, and eriochrome black T have wide range of applications, but they are lethal for all life forms [5–7]. Brilliant green is used in paper printing and coloring silk, but its effects investigated on bacteria and rats alarming destruction were noted in their renal tissues and reproductive systems, so presence of these types of organic dyes in water impose threat that is why purification and detoxification of air and water are necessary to ensure safe of human and aquatic life. As listed by US-EPA, 4-nitrophenol is a cancer-causing pollutant [8]. Researchers are continuously searching to find effective and ecofriendly ways to eradicate

these toxic dyes and metals from water [9, 10]. Different methods are in practice for eradication of dyes such as adsorption, membrane filtration, biological treatment, electrochemical treatment, photocatalytic degradation, ozonation, oxidation, chemical precipitation, and ion exchange [11]. Photocatalysis is cost-effective, environment-friendly method for removal of dyes where the photocatalysts such as NiO, TiO_2, SnO_2, ZnO, and WO_3, are used for removing dyes [4]. Development of photocatalytic technology improves the water quality [12]. With the advancement, composite materials provide an opportunity to prepare cost-effective and efficient products in limited resources [13]. Nanocomposite has gained double interest in photocatalysis due to their better light harvesting property compared to individual components. NiO-Bi_2O_3 composite is helpful to disintegrate dyes such as methyl orange and methylene blue. Composite photocatalysts also improve the problems of photocatalysed reactions such as light response and low efficiencies [14]. Bimetallic composite shows better magnetic, thermal, catalytic, and optical properties [15]. Nanocomposites of ZnO-NiO are used as photocatalysts and have better properties than their individual particles and their efficiency increases by increasing NiO concentration [4]. NiO/ZnO nanocomposite is used in transparent conducting thin films for OLED applications [16]. These composites possess great photocatalytic activity against dyes such as methylene blue and Rhodamine B [17].

In the recent past, different methods such as combustion method, coprecipitation method, and sonochemical route had been employed to synthesize NiO-ZnO composites [4, 18]. However, these methods include the used toxic precursor chemical, solvents, and reducing and stabilizing agents along with expensive instruments. Recently, nanoparticles have widely been synthesized by green method by using plant extract and microorganisms as reducing and capping agents. Among different biosynthetic methods, the use of plant extract is more advantageous due to safe handling and easy availability [19]. In this research work to synthesize NiO-ZnO NC, *D. kaki* leaves extract was used and was analyzed by SEM, XRD, EDX, FTIR, and DRS. The synthesized composite used was photodegradation of BG and 4-NP in its aqueous solution under sunlight. Mathematical equations were used for determining percentage degradation and rate constant.

2. Materials and Method

2.1. Materials. Highly pure chemicals containing nickel chloride hexahydrate, zinc chloride hexahydrate, sodium hydroxide, brilliant green, and 4-nitrophenol were purchased from Sigma-Aldrich and were used without more purification. *D. kaki* leaves extract and the working solutions were prepared in deionized water.

2.2. Preparation of Plant Leaves Extract. The collected leaves of *D. kaki* were washed with tap water along with deionized water and were dried in shade. For the extract preparation, 50 g of *D. kaki* leaves were added to a beaker containing 1000 mL distilled water and boiled for three hours. The crude extract obtained was filtered, centrifuged, and stored at 4°C.

2.3. Synthesis of NiO-ZnO NC. To make precursor salt solution, 2.24 g of nickel sulphate hexahydrate was added in 50 mL deionized water and then mixed with 20 mL of *D. kaki* extract and the pH was adjusted at 8 by adding NaOH solution. For 30 min at 60°C, the reaction mixture was heated and the gel obtained was marked as solution A. Similarly, the zinc sulphate hexahydrate solution was synthesized by dissolving 2.20 g dissolved in 50 mL deionized water and mixed with 20 mL leaves extract of *D. kaki*. The pH was maintained at 10 by adding NaOH solution and the mixture was stirred and heated (60°C) for 30 min and the gel formed was marked as solution B. To synthesize NiO-ZnO NC, both gels (solutions A and B) were mixed together and for four hours stirred at 70°C. The solid product obtained was left for overnight cooling at room temperature and was then washed thrice with distilled water. The end product was dried up in electric oven at 150°C and stored in air tight bottle of polyethylene.

2.4. Characterization. The KBr pellet was analyzed by FTIR model Nicolet 6700 (USA) in the range of 4000 to 400 cm^{-1} to identify the functional groups present on the surface of the sample. The DRS model Lambda 950 was run in between 400 and 1000 nm and band gap energy was determined through Tauc plot. The XRD pattern was recorded in the range of 20 to 80 utilizing Panalytical X-Pert Pro, where Cu source was used. The FWHM values of the diffraction peaks were used to calculate the crystallite size. The morphological analysis was carried out through SEM model 5910 (Japan) and Hitachi H7700 TEM with an accelerating voltage of 100 kV, where sample was steak with sticky carbon tape. The EDX model INCA 200 (UK) coupled with SEM was operated from elemental analysis.

2.5. Photodegradation Assay of BG and 4-NP. The photocatalytic experiments were performed second week of June, 2020, from 11 am to 3 pm. The temperature in these days was ranging from 38 to 45°C, where the UV index was lying between 9 and 12. Photocatalytic efficiency of NiO-ZnO NC was checked by the photodegradation of BG, where 20 mg of the synthesized catalyst was added to 50 mL (10 ppm) solution of dye. To ensure the dispersion of a catalyst in dye solution, we stirred mixture in dark for 30 min to the attained adsorption-desorption equilibrium. The reaction mixture was exposed to solar light and the decrease in the absorbance maxima was monitored after a specific interval of time (min). Sufficient volume of sample was analyzed via UV spectrophotometer and absorbance was decreased which was recorded as against time.

The photodegradation of 4-nitrophenol by NiO-ZnO NC was checked by taking 10 mg of NC and we added it into aqueous solution of 4-nitrophenol at room temperature. The reaction mixture was stirred for half an hour to attain adsorption-desorption equilibrium. Afterward, the reaction

was exposed to sunlight, and after regular interval, the sample was taken and centrifuged, and decrease in absorbance was checked in UV-Vis spectrophotometer by determining absorbance at 318 nm. The mathematical equations (equations (1) and (2)) were applied to determine photocatalytic reaction parameters [20].

$$\% \text{ degradation} = \frac{C_o - C_e}{C_o} \times 100, \quad (1)$$

$$\ln\left(\frac{C}{C_O}\right) = -kt. \quad (2)$$

3. Result and Discussion

3.1. FTIR Analysis. FTIR spectroscopic analysis of NiO-ZnO NC (Figure 1(a)) shows that presence of transmittance band in the range of 3591–3222 cm^{-1} shows stretching vibration of hydroxyl group attached with metal center [21]. The peak originated at 2339 cm^{-1} depicts atmospheric CO_2 adsorbed on the surface of synthesized nanocomposite [22]. The peaks at 1642 cm^{-1} and 1506 cm^{-1} are due to bending vibration of OH bond in plane and out of plane, respectively [21, 22]. The peak visible at 1379 cm^{-1} and 1116 cm^{-1} corresponds to OH group [23]. The peak at 1047 cm^{-1} region indicates Zn-O bond [22], whereas the peak appeared at 952 cm^{-1} is due to Ni-O stretching vibrations [24]. The peaks at 685 cm^{-1} and 590 cm^{-1} show nickel and zinc metal oxides, respectively [21]. The FTIR spectrum of *D. kaki*: Figure 1(b) exhibits characteristic FTIR peaks at 3466, 3010, 2971, 1715.53, 1424.33, 1357.03, 1220.84, 1092.54, 895.57, 793.91, and 529.54 cm^{-1} attributed to the stretching of O-H, C-H (aromatic), C-H (aliphatic), C = O, C = C, N-O in NO_3, C-N of primary amine, and C-X (halogen), respectively [25]. The phenolic compounds in the leaf extract of *D. kaki* are responsible for the reduction of precursor's salt and capping of the metal cation, as shown in Figure 2 [26].

3.2. DRS Analysis. Diffuse reflectance spectroscopy (DRS) is useful technique for the determination of band gap which in turn provides base of mechanism of photocatalysis. The absorbance spectrum recorded in the range of 250–1200 nm for NiO-ZnO NC is given in Figure 3, which shows maximum absorbance in the UV range. The absorbance was successively decreased with increasing wavelength suggesting that the electronic transition occurred in UV range. From the absorption edges of reflectance spectra, band gap is calculated by using Tauc plot (inset in Figure 3) by using the following equation:

$$(\alpha h\nu) = C(h\nu - Eg)^n, \quad (3)$$

where α is the absorption coefficient of material, h is Plank's constant, ν is the frequency, C is the proportionality constant, Eg is the band gap energy, and the exponent n can have values of 1/2, 2, 3/2, or 3 depending on the type of transition: direct, forbidden direct, indirect, or forbidden indirect. The optical energy band gap of NiO-ZnO NC is 3.34 eV.

3.3. SEM Analysis. SEM is a valuable technique to determine surface morphology and particle size. The low and high magnified SEM micrographs of the NiO-ZnO NC are presented in Figure 4. The micrographs show that after the dehydration, compact solid structures are formed. Several small particles with definite boundaries are seen on the surface of the hard solid structures that have no specific shape and size.

3.4. TEM Analysis. The TEM micrograph at a resolution of 70000, given in Figure 5, shows that the particles are embedded in an amorphous layer. Probably, the layer is composed of phytochemicals that exist in the aqueous extract of *D. kaki*. The majority of the particles are highly agglomerated, forming a compact structure where the boundaries between the particles are indistinguishable. However, some well-defined oval/nearly spherical particles are also seen in the image, which exhibit lucent boundaries. The particle size estimated ranges from 48.84 nm to 79.05 nm, with an average size of 63.24 nm.

3.5. XRD Analysis. The XRD data of NiO-ZnO NC are presented in Figure 6, possessing Bragg's reflections for both NiO and ZnO. The diffraction bands for NiO had appeared at 2θ position 33.19 and 59.91° corresponding to hkl values (001) and (110), respectively. These peaks corresponding to monoclinic phase of NiO are having space group C_2/m with cell constants $a = 5.11$, $b = 2.95$, and $c = 2.95$ Å as per reference card (01-072-1464). The Bragg's signals for ZnO appeared at 2θ position along with hkl values 31.74(100) and 35.74(101) attributed to hexagonal geometry of ZnO with a space group of P63mc where the cell constants are $a = 3.24$, $b = 3.24$, and $c = 5.20$ corresponding to JCPDS card (00-0361451). The XRD pattern exhibits peaks for both NiO and ZnO suggesting the formation of hetero-structure, whereas the noisy spectrum suggests the presence of some amorphous content in the sample. The Scherer formula was used to calculate the crystallite size (7.62 nm) considering the FWHM values of diffraction bands, where β is full width at half maximum and λ is the X-ray wavelength.

$$\mathbf{t} = \frac{0.9\boldsymbol{\lambda}}{\boldsymbol{\beta}\mathbf{cos}\boldsymbol{\theta}}. \quad (4)$$

3.6. EDX Analysis. The EDX is a significant technique to determine the chemical composition [27]. EDX spectrum is shown in Figure 7, which reveals that the elements within synthesized NiO-ZnO NC are nickel, zinc, oxygen, and carbon. The existence of carbon in the sample may point the use of plant during synthesis or it may also be due to the use of carbon tape during analysis. The short signal appeared at 0.2 keV is of carbon, due to the use of carbon tape during study, or might be because of plant materials. The medium band at 0.6 keV assigned to oxygen (O) is due to the formation of oxide of Ni and Zn. The signals at 0.9, 7.5, and 8.2 eV are because of nickel, whereas the bands appeared at 1, 8.6, and 9.5 eV attributed to the presence of zinc in

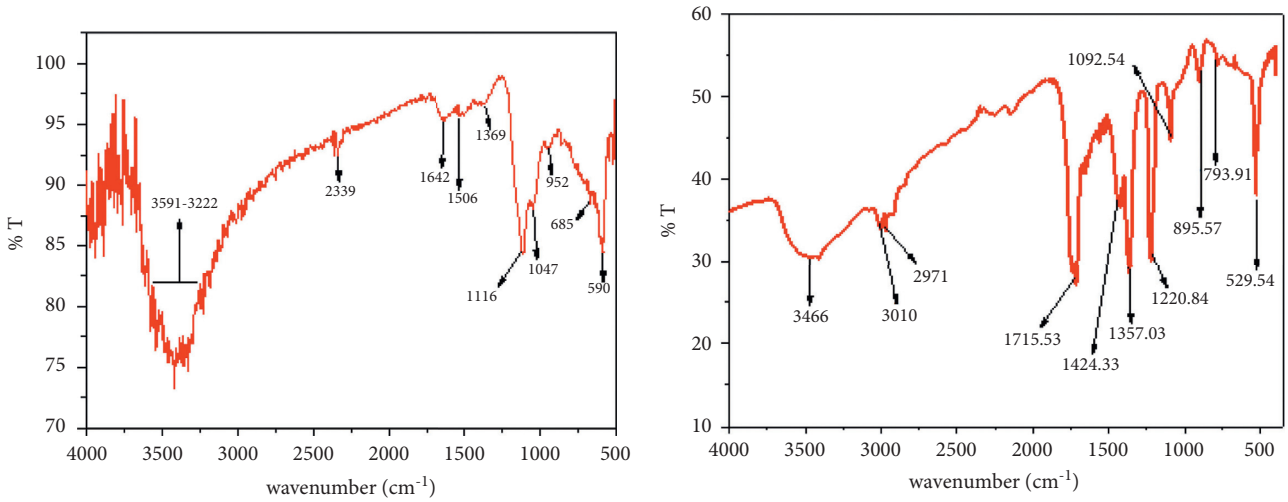

Figure 1: (a) FTIR spectrum of NiO-ZnO NC and (b) FTIR spectrum of *D. kaki*.

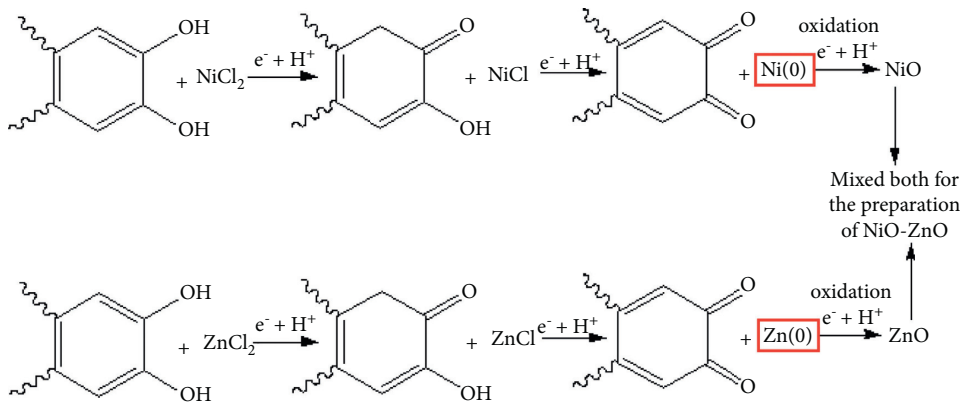

Figure 2: Proposed mechanism for the green synthesis of NiO-ZnO NC.

product. The weight percentages of carbon, nickel, zinc, and oxygen estimated by EDX analysis are 1.03, 13.98, 32.50, and 52.43%, respectively. The EDX results were found comparable with those reported by Karthikeyan et al. [28].

3.7. Photocatalytic Activity. The NiO-ZnO NC prepared by green method was used as photocatalyst for the deterioration of BG and 4-NP. Before the photocatalytic experiment, a self-photolysis experiment was carried out in the absence of catalyst, and after 90 min, a slight decrease was seen in the absorbance maxima and determined percent degradation was found to be 2.78%. To degrade, BG reaction was carried out in sun radiations during 11 am to 2 pm. For the photocatalytic experiment, 20 mg of catalyst was added into 50 mL of BG solution (10 ppm) and stirred in dark for 30 min for establishing adsorption-desorption equilibrium [20]. After that, the mixture was placed under sunlight, and with the passing time, the decrease in the absorbance maxima was noted, as shown in Figure 8(a). Similar procedure was repeated for 4-NP and the results obtained are given in Figure 9(a). The activity of pure NiO-ZnO NC was checked in terms of percentage degradation, which was calculated by applying equation (2). The percentage degradation of BG was determined to be 92.5% after 90 min (Figure 8(b)), whereas 69.7% of the 4-NP was degraded in 45 min, as shown in Figure 9(b). The kinetics for the photocatalytic reaction was determined by using Langmuir–Hinshelwood equation (equation (2)) and the straight line obtained (Figures 8(c) and 9(d)) suggest the reaction follows pseudofirst order and the determined rate constant is 2.8×10^{-2} min^{-1} and 1.13×10^{-2} min^{-1} for BG and 4-NP, respectively. The stability/reusability of the NiO-ZnO NC was checked by addition of fresh BG solution into the reactor under same reaction condition. The process was repeated for four times under the same condition, and the data obtained are shown in Figure 7(d), which shows during the initial experiment, the mineralization rate was high and a gradual reduction was seen in afterward cycles. The percent degradation was recorded to be 92.52, 90.38, 87.69, and 84.30% during 1st, 2nd, 3rd, and 4th cycles, respectively. This shows the stability of the synthesized NiO-ZnO NC and can be used for several

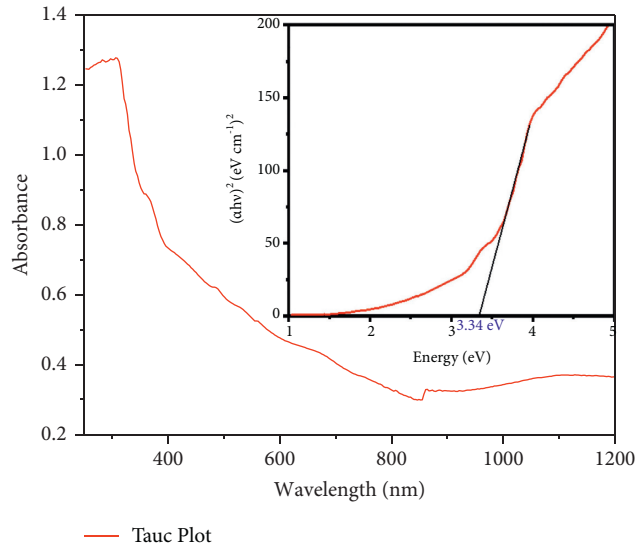

Figure 3: DRS spectrum (inset: Tauc plot) of NiO-ZnO NC.

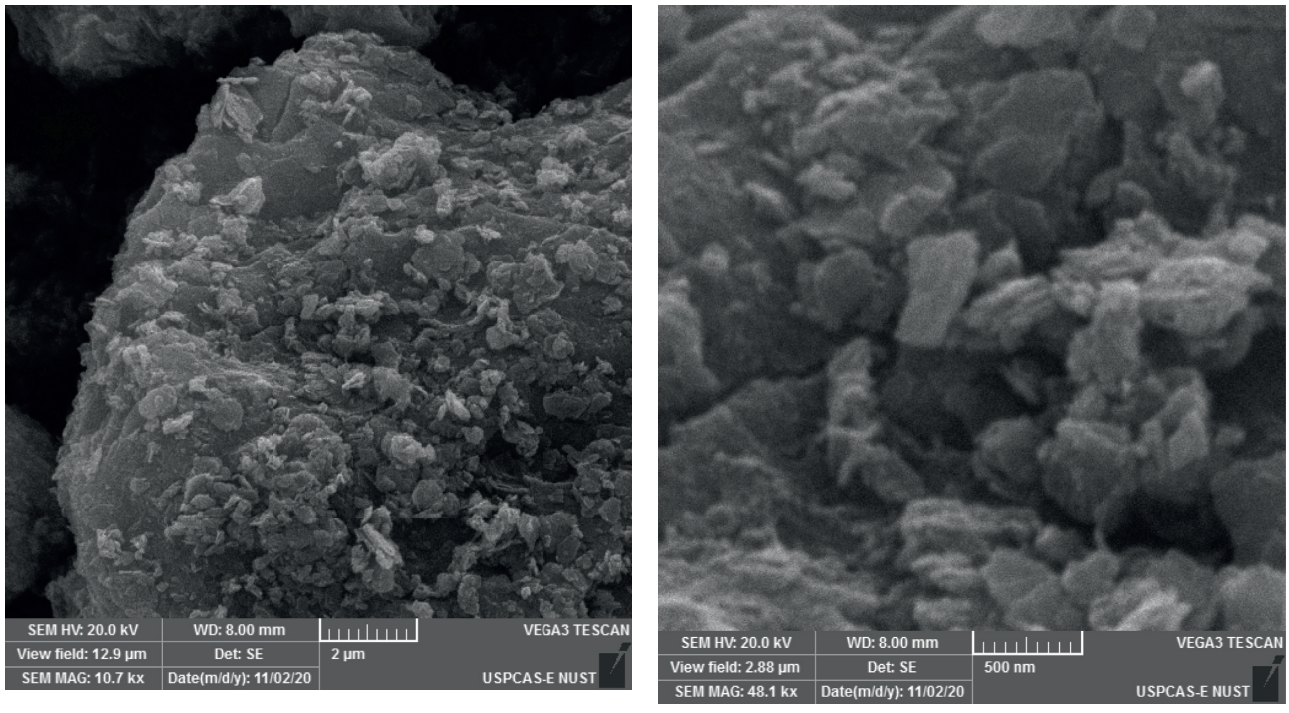

(a) (b)

Figure 4: Low (a) and high (b) magnification SEM micrographs of NiO-ZnO NC.

step degradations of organic pollutants. The photocatalytic activity of synthesized NiO-ZnO NC was compared against other organic dyes, as shown in Table 1.

When solar radiations having energy equal or greater than catalyst's band gap fall on NiO-ZnO NC surface, valence electrons of both oxides of nickel and zinc get excited to the conduction band and positive holes get created in the valance band. The photo-generated electrons from conduction band of NiO get transferred to the conduction band of ZnO, whereas the positive holes get shifted from ZnO to NiO, thus keeping the electrons and holes apart as shown in Figure 10 [29]. Photo-generated holes react with the water or surface hydroxyl group and form hydroxyl radical and photo-induced electrons produce superoxide anion by reacting with oxygen which by further reaction produces hydroxyl radicals. These hydroxyl radicals degrade

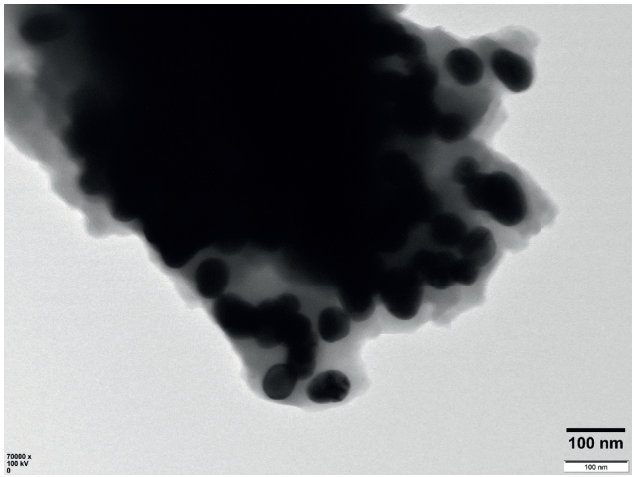

Figure 5: TEM micrograph of NiO-ZnO NC.

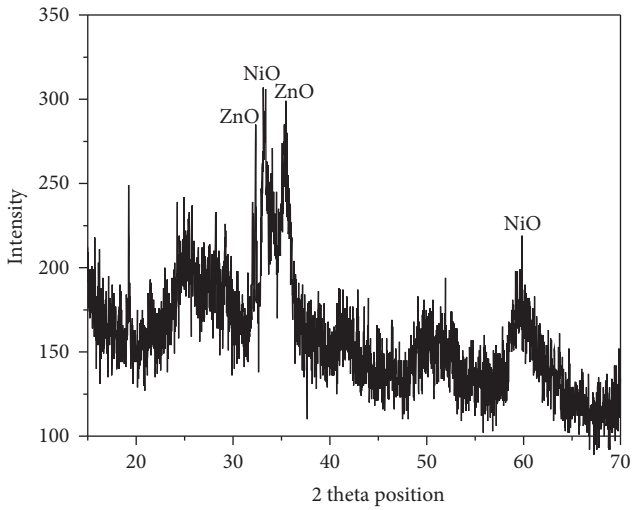

Figure 6: X-ray diffractogram of NiO-ZnO NC.

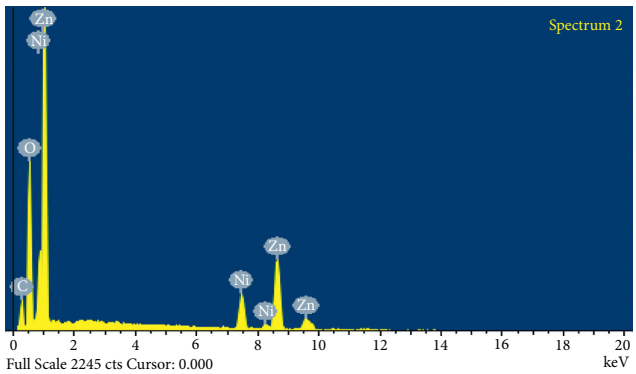

Figure 7: EDX spectrum of NiO-ZnO NC.

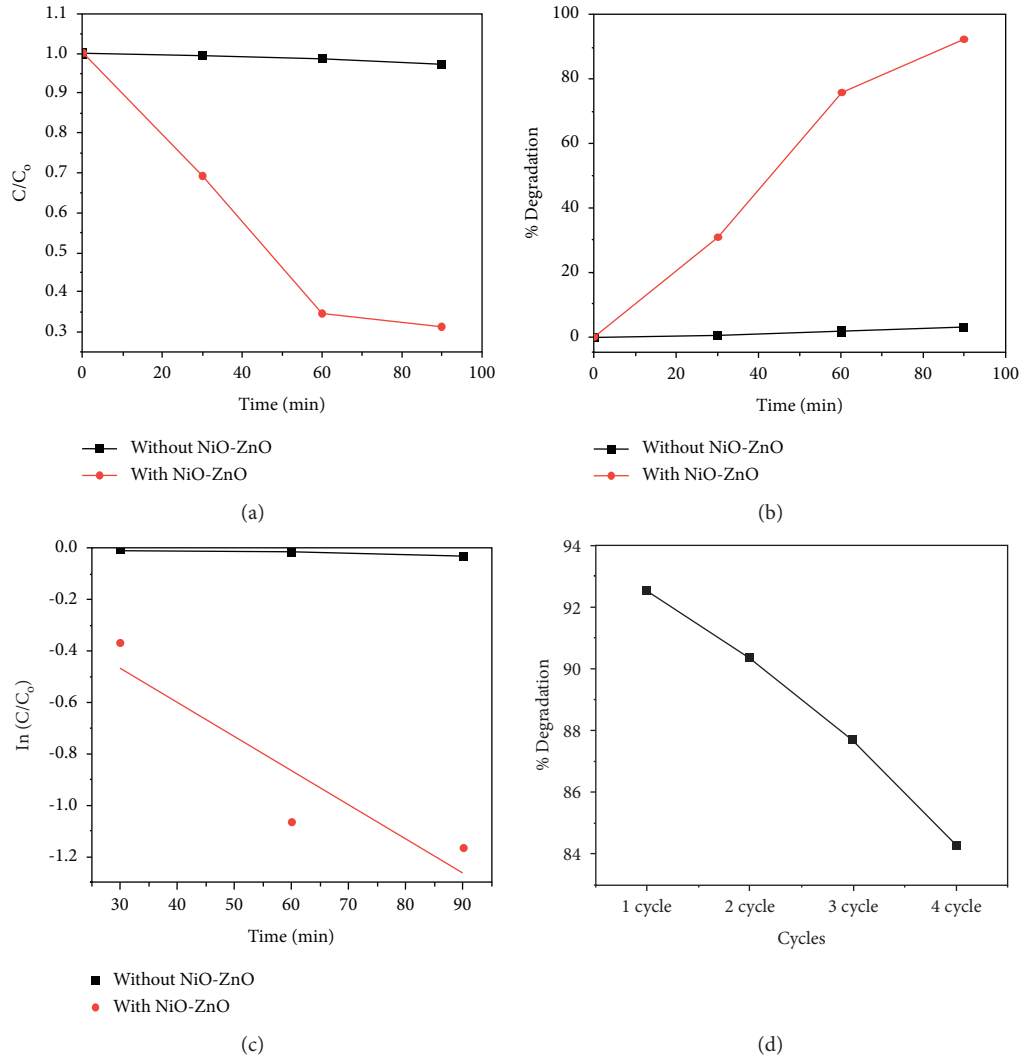

Figure 8: Photodegradation of BG. (a) Degradation profile, (b) percent degradation, (c) kinetic isotherm, and (d) reusability data.

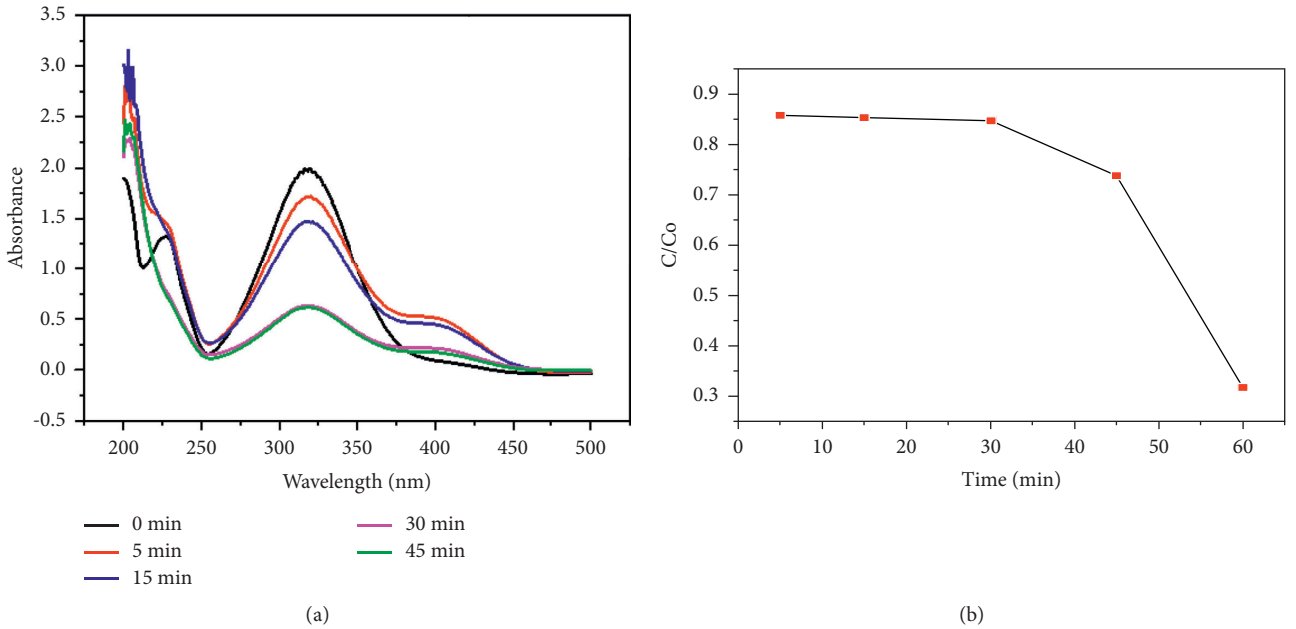

Figure 9: Continued.

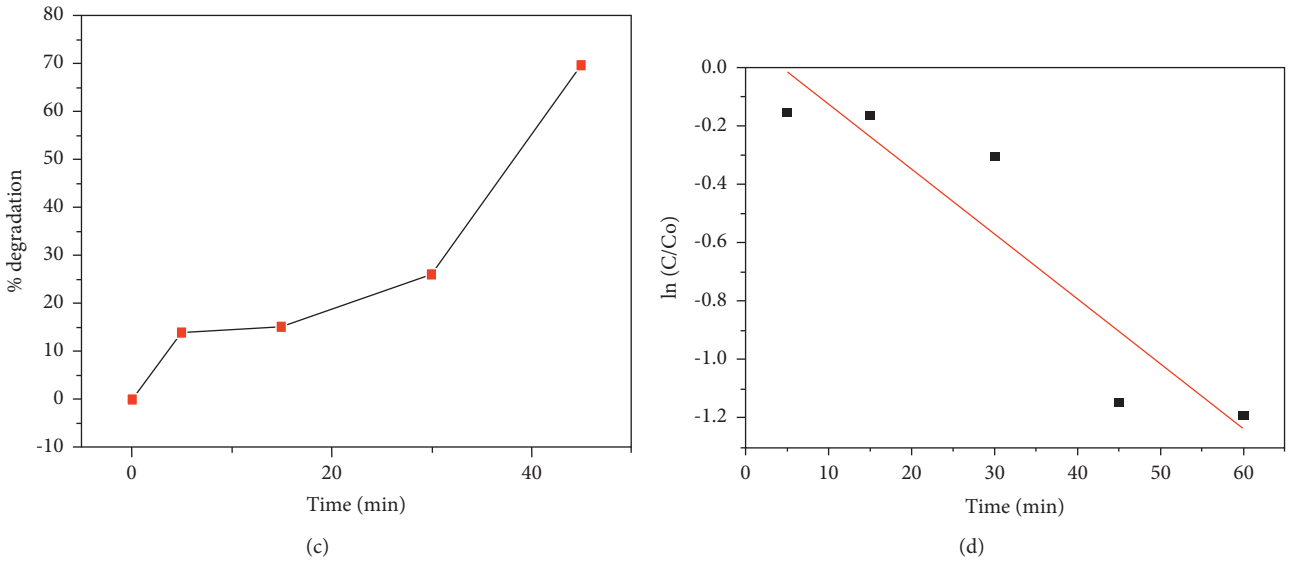

Figure 9: (a) Absorption spectra of 4-nitrophenol. (b) Degradation profile, (c) percent degradation, and (d) kinetic isotherm.

Table 1: The photocatalytic efficacy of NiO-ZnO NC against different organic pollutants.

S. no.	Nanocatalysts	Time (min)	Percentage degradation	References
1	Rhodamine B	120	70	[17]
2	Rhodamine 6G	390	92.8	[31]
3	Methyl orange	150	91.89	[32]
4	Eriochrome black T	90	83.36	[33]
5	Methylene blue	120	65	[17]
6	Brilliant green	90	92.5	Present work
7	4-Nitrophenol	45	69.7	Present work

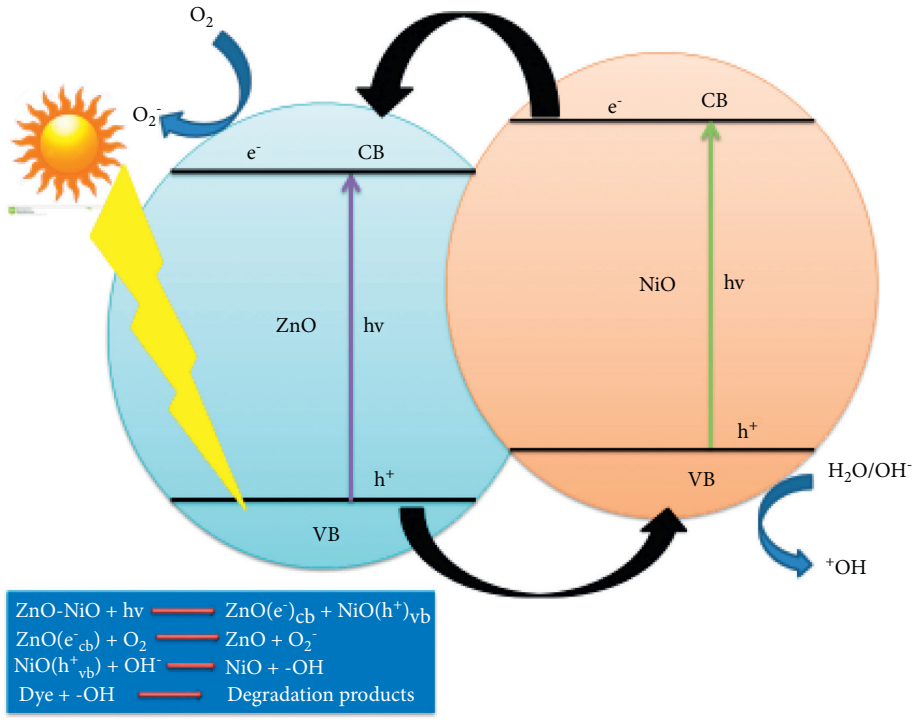

Figure 10: Schematic representation of electron flow during photocatalysis.

the dye and convert it into harmless substances [30]. The set of chemical reaction given in Figure (10) summarizes the hole-electron shifting and degradation of BG and 4-NP.

4. Conclusion

To synthesize NiO-ZnO NC, green method was found to be a very efficient, fast, and economical process. FTIR and EDX confirmed the formation of binary nanocomposite. The XRD analysis shows that amorphous content was also present along with crystalline phase and also confirms the formation of hetero-structure. The band gap calculated from DRS for NiO-ZnO was different from their individual nanoparticles which confirm the formation of new material. SEM reveals the roughness and agglomeration of particles after dehydration. The photocatalytic degradation of NiO-ZnO NC was checked against BG and 4-NP, which reveals that under the applied conditions, the NiO-ZnO NC shows marvelous photocatalytic performance and could be used in the future for waste water treatment on large scale.

Data Availability

The data used to support the findings of this study are included within the article.

Conflicts of Interest

The authors declare that they have no conflicts of interest.

Acknowledgments

The authors are grateful to the Deanship of Scientific Research for funding this article by Taif University Researchers Supporting Project number (TURSP-2020/28), Taif University, Taif, Saudi Arabia.

References

[1] P. Rasheed, S. Haq, M. Waseem, S. U. Rehman, and W. Rehman, "Green synthesis of vanadium oxide-zirconium oxide nanocomposite for the degradation of methyl orange and picloram," *Materials Research Express*, vol. 7, no. 2, pp. 1–8, 2020.

[2] M. Kaykhaii, M. Sasani, and S. Marghzari, "Removal of dyes from the environment by adsorption process," *Chemical and Materials Engineering*, vol. 6, no. 2, pp. 31–35, 2018.

[3] R. Jeyachitr, N. Sriharan, V. Senthilnathan, and T. Senthil, "Effect of Ni doping on structural, optical and photocatalytic properties of Zn1-XNiXO nanoparticles prepared by different pH conditions," *Journal of Advances in Chemistry*, vol. 12, no. 6, pp. 4097–4107, 2017.

[4] U. S. Udayachandran Thampy, A. Mahesh, K. S. Sibi, I. N. Jawahar, and V. Biju, "Enhanced photocatalytic activity of ZnO-NiO nanocomposites synthesized through a facile sonochemical route," *SN Applied Sciences*, vol. 1, no. 11, pp. 1–15, 2019.

[5] M. A. Aly-Eldeen, A. A. M. El-Sayed, D. M. S. A. Salem, and G. M. El Zokm, "The uptake of eriochrome Black T dye from aqueous solutions utilizing waste activated sludge: adsorption process optimization using factorial design," *The Egyptian Journal of Aquatic Research*, vol. 44, no. 3, pp. 179–186, 2018.

[6] J. Šíma and P. Hasal, "Photocatalytic degradation of textile dyes in aTiO2/UV system," *Chemical Engineering Transactions*, vol. 32, pp. 79–84, 2013.

[7] S. M. Hassan and M. A. Mannaa, "Photocatalytic degradation of brilliant green dye by SnO_2/TiO_2 nanocatalysts," *International Journal of Nano and Material Sciences*, vol. 5, pp. 9–19, 2016, Journal Homepage: https://www.ModernScientificPress.Com.

[8] V. Yadav, P. Verma, H. Sharma, S. Tripathy, and V. K. Saini, "Photodegradation of 4-nitrophenol over B-doped TiO_2 nanostructure: effect of dopant concentration, kinetics, and mechanism," *Environmental Science and Pollution Research*, vol. 27, no. 10, pp. 10966–10980, 2020.

[9] R. Rehman, S. J. Muhammad, and M. Arshad, Brilliant Green and Acid Orange 74 Dyes Removal from Water by Pinus Roxburghii Leaves in Naturally Benign Way : An Application of Green Chemistry, 2019, 2019.

[10] S. Shoukat, W. Rehman, S. Haq, M. Waseem, and A. Shah, "Synthesis and characterization of zinc stannate nanostructures for the adsorption of chromium (VI) ions and photo-degradation of rhodamine 6G," *Materials Research Express*, vol. 6, no. 11, p. 115052, 2019.

[11] A. Ahmad, S. H. Mohd-Setapar, C. S. Chuong et al., "Recent advances in new generation dye removal technologies: novel search for approaches to reprocess wastewater," *RSC Advances*, vol. 5, no. 39, pp. 30801–30818, 2015.

[12] M. Pawar, S. T. Sendo, and P. Gouma, Review Article A Brief Overview of TiO_2 Photocatalyst for Organic Dye Remediation : Case Study of Reaction Mechanisms Involved in Ce-TiO_2 Photocatalysts System, 2018, 2018.

[13] L. Singh, G. Goga, and M. K. Rathi, "Latest developments in composite materials," *IOSR Journal of Engineering*, vol. 02, no. 8, pp. 152–158, 2012.

[14] A. Hameed, V. Gombac, T. Montini, M. Graziani, and P. Fornasiero, "Synthesis, characterization and photocatalytic activity of NiO-Bi_2O_3 nanocomposites," *Chemical Physics Letters*, vol. 472, no. 4-6, pp. 212–216, 2009.

[15] G. Sharma, A. Kumar, S. Sharma et al., "Novel development of nanoparticles to bimetallic nanoparticles and their composites: a review," *Journal of King Saud University Science*, vol. 31, no. 2, pp. 257–269, 2019.

[16] M. Vimal Kumar, T. S. Gokul Raja, N. Selvakumar, and K. Jeyasubramanaian, "Synthesis and characterization of NiO-ZnO nanocomposite by a cost efficient self-combustion technique," *Journal of Achievements in Materials and Manufacturing Engineering*, vol. 79, no. 1, pp. 13–18, 2016.

[17] M. Hassanpour, H. Safardoust-Hojaghan, and M. Salavati-Niasari, "Rapid and eco-friendly synthesis of NiO/ZnO nanocomposite and its application in decolorization of dye," *Journal of Materials Science: Materials in Electronics*, vol. 28, no. 15, pp. 10830–10837, 2017.

[18] S. Kerli and Ü. Alver, "Preparation and characterisation of ZnO/NiO nanocomposite particles for solar cell applications," *Journal of Nanotechnology*, vol. 2016, Article ID 4028062, 5 pages, 2016.

[19] S. Taheriniya and Z. Behboodi, "Comparing green chemical methods and chemical methods for the synthesis of titanium dioxide nanoparticles," *International Journal of Pharmaceutical Sciences and Research*, vol. 7, pp. 4927–4932, 2016.

[20] N. Bibi, S. Haq, W. Rehman et al., "Low temperature fabrication of SnO_2, ZnO and Zn_2SnO_4 nanostructures for the degradation of Rhodamine 6G: characterization," *Biointerface Research in Applied Chemistry*, vol. 10, pp. 5895–5900, 2020.

[21] K. Velmurugan, V. S. K. Venkatachalapathy, and S. Sendhilnathan, "Synthesis of nickel zinc iron nanoparticles by coprecipitation technique," *Materials Research*, vol. 13, no. 3, pp. 299–303, 2010.

[22] S. A. Khan, S. B. Khan, L. U. Khan, A. Farooq, K. Akhtar, and A. M. Asiri, "Fourier transform infrared spectroscopy: fundamentals and application in functional groups and nanomaterials characterization," *Handbook of Materials Characterization*, vol. 1, pp. 317–344, 2018.

[23] S. Nagarajan and K. Arumugam Kuppusamy, "Extracellular synthesis of zinc oxide nanoparticle using seaweeds of gulf of Mannar, India," *Journal of Nanobiotechnology*, vol. 11, no. 1, p. 39, 2013.

[24] A. O. Juma, E. A. A. Arbab, C. M. Muiva, L. M. Lepodise, and G. T. Mola, "Synthesis and characterization of CuO-NiO-ZnO mixed metal oxide nanocomposite," *Journal of Alloys and Compounds*, vol. 723, pp. 866–872, 2017.

[25] A. Attar and M. Altikatoglu Yapaoz, "Biosynthesis of palladium nanoparticles using *Diospyros kaki* leaf extract and determination of antibacterial efficacy," *Preparative Biochemistry & Biotechnology*, vol. 48, no. 7, pp. 629–634, 2018.

[26] S. Haq, F. Abbasi, M. Ben Ali et al., "Green synthesis of cobalt oxide nanoparticles and the effect of annealing temperature on their physiochemical and biological properties," *Materials Research Express*, vol. 8, no. 7, Article ID 075009, 2021.

[27] M. M. Sajid, S. B. Khan, N. A. Shad, and N. Amin, "Synthesis of $Zn_3(VO_4)_2/BiVO_4$ heterojunction composite for the photocatalytic degradation of methylene blue organic dye and electrochemical detection of H_2O_2," *RSC Advances*, vol. 8, no. 62, pp. 35403–35412, 2018.

[28] V. Karthikeyan, A. Padmanaban, T. Dhanasekaran et al., "Synthesis and characterization of ZnO/NiO and its photocatalytic activity, mechanics," *Materials Science & Engineering*, vol. 9, pp. 1–5, 2017.

[29] S. Haq, S. Shoukat, W. Rehman, M. Waseem, and A. Shah, "Green fabrication and physicochemical investigations of zinc-cobalt oxide nanocomposite for wastewater treatment," *Journal of Molecular Liquids*, vol. 318, Article ID 114260, 2020.

[30] A. Shah, S. Haq, W. Rehman, M. Waseem, S. Shoukat, and M.-u. Rehman, "Photocatalytic and antibacterial activities of *Paeonia emodi* mediated silver oxide nanoparticles," *Materials Research Express*, vol. 6, no. 4, Article ID 045045, 2019.

[31] S. Shoukat, S. Haq, W. Rehman et al., "Remediation of chromium (VI) and rhodamine 6G via mixed phase nickel-zinc nanocomposite: synthesis and characterization," *Journal of Inorganic and Organometallic Polymers and Materials*, vol. 31, no. 4, pp. 1565–1575, 2020.

[32] J. Li, F. Zhao, L. Zhang et al., "Electrospun hollow ZnO/NiO heterostructures with enhanced photocatalytic activity," *RSC Advances*, vol. 5, no. 83, pp. 67610–67616, 2015.

[33] M. Karimi-Shamsabadi, M. Behpour, A. K. Babaheidari, and Z. Saberi, "Efficiently enhancing photocatalytic activity of NiO-ZnO doped onto nanozeoliteX by synergistic effects of p-n heterojunction, supporting and zeolite nanoparticles in photo-degradation of Eriochrome Black T and Methyl Orange," *Journal of Photochemistry and Photobiology A: Chemistry*, vol. 346, pp. 133–143, 2017.